Makaremi M, Lim CX, Pasbakhsh P, Lee SM, Goh KL, Chang HK, Chan ES.
Electrospun functionalized polyacrylonitrile-chitosan Bi-layer membranes for water filtration applications.
***RSC Advances* 2016, 6(59), 53882-53893.**

Electrospun Functionalized Polyacrilonitrile-Chitosan Bi-layer Membranes for Water Filtration Applications

Maziyar Makaremi [a], Pooria Pasbakhsh [a]*, Lee Sui Mae [b], Chia Xin Lim [b], K.L. Goh [c], Hengky Chang [d]

[a] Mechanical Engineering Discipline, School of Engineering, Monash University Malaysia, 47500 Selangor, Malaysia

[b] School of Science, Monash University Malaysia, 47500 Selangor, Malaysia

[c] School of Mechanical and Systems Engineering, Newcastle University, NE1 7RU, United Kingdom

[d] Nanotechnology and Materials Science, Biomedical Engineering Group, School of Engineering (Manufacturing), Nanyang Polytechnic, Singapore, 569830, Singapore

KEYWORDS

Structural hierarchy, Mechanical properties, Zinc Oxide nanoparticles, Antibacterial, Heavy metal adsorption

ABSTRACT

Water scarcity has become one of the global systemic risks, prompting the development of more efficient filtration technology. Recently, increased attention has been given to low cost membrane materials such as polyacrylonitrile (PAN) nanofibrous mesh for water filtration. In this study, electrospun PAN nanofibrous membranes were functionalized with zinc oxide (ZnO) nanoparticles and coated with a layer of electrospun chitosan (Cs), in order to improve the mechanical properties, and anti-bacterial and water filtration performance of the membrane. Morphological analysis revealed that the PAN/ZnO-Cs membrane featured a structural hierarchy comprising a layer of highly porous structure of nanofibrous PAN membranes and a less fibrous and thinner layer of Cs coating. Addition of the Cs layer increases the tensile strength and elastic modulus of the membranes. Results acquired from water permeability test indicated that the bi-layer membranes possessed adequate transport properties for typical membrane applications. The additional Cs layer and ZnO nanoparticles significantly improved the heavy metal ion adsorption performance of the PAN membranes. The efficiency of the membrane for bacteria filtration, parameterizes by the log reduction value, for PAN/ZnO-Cs membranes is 2 orders of magnitude higher than PAN membranes; the efficiency of the membrane for antibacterial action (i.e. in terms of log reduction value) for the former is 6 orders of magnitude higher than the latter. These results indicate the PAN/ZnO-Cs membranes are structurally more stable than PAN membranes, better at bacteria removal during the filtration process and better at self-cleaning (i.e. membrane biofouling resistance) than PAN membranes, signifying the potential of these membranes for water filtration applications.

INTRODUCTION

The demand for clean drinking water is fundamental for human life and it has sparked immense interest in production of high efficient filtration devices which employ advanced functional nanosized materials such as nanofibers. Electrospinning, a simple and cost effective method, has been extensively used to produce nanofibrous filtration membranes with small pore size, large pore volumes and excellent mechanical stability [1,2]. Nanofibrous filtration membranes are made of randomly laid nano-sized fibers which can effectively filter out particles by the size exclusion mechanism [3]. Furthermore, incorporation of specific functionality on the surface of these membranes extends their ability to perform a one step removal of microorganisms and chemical compounds along with sized-based separation [4].

Electrospun polyacrilonitrile (PAN) nanofibrous membranes find applications in many areas such as electrically conductive nanofibers, wound dressing, biocatalyst, tissue scaffolding, and drug delivery systems [5]. High chemical resistance, thermal stability and wetability of PAN nanofibers [6] have led to their extensive use as ultrafiltration [7] and nanofiltration [8] membranes. However, incorporation of functional chemicals and polymers is required in order to enhance their performance for heavy metals adsorption and removal of microorganisms.

Chitosan (Cs) is the derivate of chitin (the second most abundant biological polysaccharide). Chitosan has received a considerable attention due to its unique properties such as biodegradability and non-toxicity as well as heavy metal ion adsorption and antibacterial performance. Owing to these exceptional properties, chitosan finds applications in many areas such as food preservation, wound dressing, drug delivery and biosensors [9–13]. Furthermore, Several studies have been done on inherent antimicrobial character of chitosan exerted towards bacteria and viruses for water filtration application [14,15]. It has been reported that electrospinnability of chitosan has been restricted due to its polycationic nature in solution, rigid chemical structure and specific inter and intra-molecular interactions [16]. Therefore, addition of a synthetic biodegradable polymer such as poly(vinyl alcohol) (PVA) [17] or poly(ethylene oxide) (PEO) [18] to the chitosan solution can improve the electrospinnability of chitosan, leading to formation of nanofibrous membranes containing high degree of chitosan nanofibers.

Electrospun composite chitosan membranes with high antibacterial and adsorption properties have been extensively studied for water filtration applications. In most cases, chitosan has been used as a coating layer on the surface of a non-woven membrane of a synthetic polymer with high mechanical stability. For instance, Desai *et al.* [14] fabricated nanofibrous filter media by electrospinning of chitosan/PEO blend solutions onto a spunbonded non-woven polypropylene substrate. Results indicated 2–3 log reduction in bacterial colonization of *Escherichia coli* after 6 hours of contact time. In another study, Cooper *et al.* [19] reported that chitosan/polycaprolactone(PCL) fibrous membranes significantly reduced *Staphylococcus aureus* bacterial colonization compared to PCL fibrous membranes. Furthermore, Haider *et al.* [20] investigated the heavy metal ion adsorption performance of chitosan nanofibrous membranes. Results indicated the highly effective performance of the membranes in adsorption of toxic metal ions such as Cu(II) and Pb(II) .

Recently, there have been several reports on the incorporation of metallic and metal oxide materials into electrospun polymers for improving the antibacterial performance [21–23]. These inorganic materials have attracted particular interest due to their stability in harsh processes and minimal toxicity [24]. For instance, Dasari *et al.* [25] reported on the fabrication of electrospun polylactic acid (PLA) membranes embedded with Ag and Cu. Antibacterial action of the membranes were characterized using *Saccharomyces cerevisiae* bacteria; the findings reported that the membrane has an appreciable effect on the bacterial, reducing the bacteria population by 85%. Metal oxides, such as ZnO, possess bactericidal properties and can inhibit both gram-positive and gram-negative bacteria [26,27]. Hwang *et al.* [28] evaluated the antibacterial action of electrospun ZnO~~/TiO$_2$~~ composite fibrous membrane and found that the presence of ZnO nanoparticles on the surface of the nanofibres exhibited appreciable antibacterial effects against gram-negative *Escherichia coli* and gram-positive *Staphylococcus aureus*. Moreover, since ZnO can facilitate a high amount of surface active sites for adsorption of heavy metal ions from an aqueous solution, it is a promising candidate for the removal of contaminants from the environment [29]. For instance, ZnO nano-sheets that have been prepared via a hydrothermal approach exhibit good sorption capacity for Pb^{2+} due to presence of surface hydroxyl groups (Ma *et al.* [30]).

Here we report on a study to synthesize electrospun PAN-Cs bi-layer fibrous membranes coated with ZnO nanoparticles. Chemical structure and morphological properties of the fibrous membranes were examined by field emission scanning electron microscope (FE-SEM), scanning transmission electron microscope (STEM), Fourier transform infrared spectroscopy (FTIR) and X-ray diffraction (XRD). Mechanical properties of the fibrous membranes were investigated by tensile tests while the membrane capacity for heavy metal ion adsorption was evaluated by inductive coupled plasma-optical emission spectrophotometer (ICP-OES). Both bacteria filtration and anti-bacterial performance of the membranes were evaluated by antibacterial assays. The permeability of the membranes was measured by water flow permeability tests.

EXPERIMENTAL

Materials

Polyacrylonitrile (Mw=150 KDa), chitosan (Mw=50KDa) with 75 - 85% DD and Poly(ethylene oxide) (Mw = 900 KDa) were purchased from Sigma Aldrich. Zinc oxide (Zano®20) was donated by Umicore. The spinning solvent dimethyl sulfoxide (DMSO) was purchased from Fischer Scientific while acetic acid was purchased from R&M Chemicals.

Preparation of electrospun nanofibrous membranes

In order to make an 8 w/w % PAN solution, 0.86 g of polymer pellets were dissolved in 10 ml of 99.6% DMSO and stirred for 6 hours until the solution became homogenous. Furthermore, 5 w/w% ZnO were added to the PAN solution and stirred for 6 hours in order to make PAN/ZnO solution. The PAN and PAN/ZnO solutions were electrospun onto a rotating drum (300 rpm) via an electrospinning device (NB-EN1, NanoBond), containing a metallic needle, a feed pump and a high voltage power supply. These solutions were electrospun with flow rate of 1.4 mL/hr, having distance of 15 cm and voltage that ranged from 13 to 14 kV. Furthermore, 3g of chitosan powder and 3g of PEO powder were separately added to 50% (v/v) acetic acid and stirred for 24 hours, resulting in a 3% (w/v) chitosan and 3% (w/v) PEO solution. These solutions were mixed

together in chitosan/PEO ratio of (70:30) and then electrospuned on PAN and PAN/ZnO membranes for 1.5 hours with flow rate of 0.2 mL/hr, distance from rotating collector of 10 cm and voltage of 17-18 kV. Schematic drawing of PAN/Cs/ZnO membrane has been shown in Figure 1.

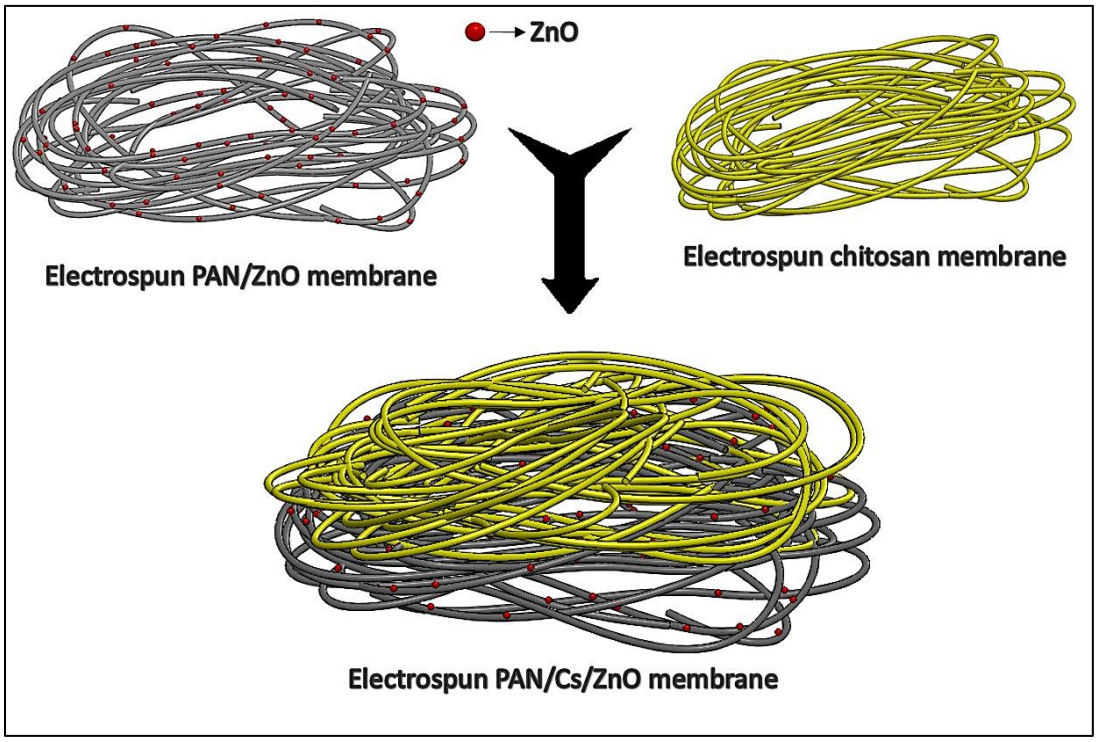

Figure 1. Schematic diagram of the structural hierarchy of the PAN/ZnO-Cs bi-layer membrane

Characterization of membranes

Morphology analysis

The morphologies of electrospun membranes were observed under ultra-high resolution field emission scanning electron microscope (FE-SEM, Hitachi SU8010). To prevent electrostatic charging during observation, the samples were coated with a thin layer of platinum. Fiber diameter and porosity of the membranes were measured by Image J analysis software.

Tensile analysis

Mechanical properties of the membranes were calculated by a strip tensile test technique based on the ASTM D882-02 standard. Each film was cut into strips (10.0×2.5 cm) and stretched to break at rate of 2 mm/min suing a TA XT PlusTexture Analyzer (Stable Micro System, UK). The width and the thickness of the samples (which varied between 0.016 to 0.04 mm) were used to determine the nominal cross-sectional area of the respective samples. Statistical analysis (commercial software SPSS, v.18) was carried out using One-way analysis of variance (ANOVA) together with Turkey's post hoc test to evaluate for differences in the mechanical properties among the four different membranes, namely PAN, PAN/ZnO, PAN-Cs and PAN/ZnO-Cs. A test was regarded as significance when the $p<0.05$. In the discussion that follows, where appropriate, we may use the mean ± standard deviation when stating the results.

Fourier transform infrared (FTIR) analysis

FTIR spectroscopy (Thermo Scientific IS10) was conducted to identify the chemical interactions occurring inside the electrospun membranes and the chemical compositional homogeneity of the samples. All spectra were obtained for wavelengths of 600 to 4000 cm^{-1} with 32 scans per specimen at 0.4 cm^{-1} resolution.

X-ray diffraction (XRD) analysis

To investigate the crystalline structure of the electrospun samples, X-ray diffraction (XRD) of both powder and membrane samples was carried out using the D8 Discover X-ray diffractometer (Bruker, Germany) with nickel-filtered Cu (Kα) radiation. The data were collected at 0.02 intervals, with counting for 0.5 seconds at each step (I am not sure what 'counting for 0.5 seconds at each step' means..) in the 2θ range of 5-60º at 40 KV and 40 mA.

Water flux and porosity measurement

Membrane permeability versus feed pressure was characterized through a pure water dead-end filtration module (Syringe Filter Holder 25 mm, Sartorius). The dried electrospun membrane was placed in the membrane module and the water was passed through by applying feed pressures between 19-157 KPa with an increment of 20 KPa. Permeation flux was calculated by:

$$J = Q / [A \quad t] \tag{1}$$

where J is the permeation flux ($L.m^{-2}h^{-1}$), Q is the permeation volume (L) of the testing solution, A is the effective area of the tested substrate (m^2) and Δt is the sampling time (h).

In order to measure the porosity of the electrospun membranes, superficial water (i.e. the excess water on the membrane surface) was blotted off from them after they have been impregnated in the water. These membranes were then weighed and dried in an air-circulating oven at 50 °C for 5 hours before measuring the dry weight. The porosity of the membranes was calculated using the following equation:

$$P = 100 \quad [W_0 \quad W_1] / \{Ah\} \tag{2}$$

where P is the membrane porosity (%); W_0 and W_1 are the masses (g) of the wet and dry membranes, respectively; A is the membrane surface area (cm^2) (is this 'A' the same as in Equation 1?); h is the membrane thickness (cm). The membrane porosity of each sample was measured several times and the results were reported as an average [31].

Heavy metal adsorption

In Cr(III) adsorption test, 10 mg of $CrK(SO_4)_2 \cdot 12H_2O$(Sigma-Aldrich) was mixed in 1 liter of deionized water. A 10 mL aliquot of Cr(III) solution was driven through electrospun membranes with thickness ranging from 0.042 to 0.072 mm at a rate of 1 mL/min using a syringe pump. The Cr(III) concentrations of the feed solution and permeate filtrate were determined by inductive coupled plasma-optical emission spectrophotometer (ICP-OES Perkin Elmer Optima 8000). Total concentration rejection (R) in adsorption of Cr(III) was given by

$$R = 100 \quad [C_f \quad C_p] / C_f \qquad (3)$$

where C_f and C_p represent the Cr (III) concentrations (CFU/ml) of the feed solution and permeate filtrate, respectively.

Bacteria filtration

Gram negative bacteria *Escherichia coli* (*E. coli* ATCC 29522) and Gram positive bacteria *Enterococcus faecalis* (*E. faecalis* ATCC 29212) were used for inoculation of the "influent" water sample. *E. coli* and *E. faecalis* are often used as indicators of human and animal fecal contamination of water. Bacteria were cultured in Luria-Bertani broth (LB) for 24 hours aerobically at 37 °C. To remove any residual growth medium, bacteria cultures were centrifuged at 10000 x *g* (?) for 1 minute, supernatant was discarded and pellet was resuspended in autoclaved distilled water. These washing processes were repeated twice to remove any remaining nutrients from the culture medium. The pellet was adjusted to 0.5 McFarland Standard (OD of 0.08-0.10 at 625nm) which corresponds to a bacterial concentration of $\sim 10^7$ colony forming units (CFU/ml). Bacteria filtration performances of all membranes were evaluated according to Daels *et al.* [32] with some modifications. Each membrane with thickness ranging from 0.042 to 0.072 mm was cut into circle with 25 mm diameter and sterilized under UV light for 30 minutes, while filter holder (syringe filter holder 25 mm, Sartorius) was autoclaved for 15 min at 121 °C. Membranes were fitted into filter holders and preconditioned by passing 3 mL of sterile distilled water. Next, 3 mL of bacterial suspension was filtered through the membranes using a syringe pump. The filtrate was then serially diluted with sterile distilled water up to 10^{-8} concentration. Viable counts were determined by spread plating on Luria-Bertani agar and incubated overnight at 37 °C aerobically. All measurements were performed in triplicate. The bacterial retention ratio was calculated in terms of *LRV* (Log Reduction Value) defined as

$$LRV = \log(C_f / C_p). \qquad (4)$$

Furthermore, the morphology of trapped bacteria was investigated using a field emission scanning electron microscope (FE-SEM, Hitachi SU8010). Bacterial cells were fixed to the

membrane with 2.5 % (v/v) glutaraldehyde in sterile phosphate buffer saline (PBS) for six hours. The fixed bacterial cells on the membrane were then serially dehydrated with 20% (v/v) ethanol in sterile distilled water, followed by 40, 60, 70, 80, 90 and 95% (v/v) ethanol in sterile distilled water and lastly with absolute ethanol for 10 minutes each.

Antibacterial performance of the membranes

To examine the antibacterial properties of electrospun membranes, *E. coli* ATCC 25922 was cultured in Luria-Bertani broth (LB) at 37°C for 24 hours. Bacteria were washed twice with sterile distilled water and adjusted to OD of 0.08-0.10 at 625 nm, which corresponds to a bacterial concentration of $\sim 10^7$ colony forming units (CFU/ml). Membranes having thickness between 0.017 to 0.035 mm were cutted into square pieces of 20 x 20 mm and sterilized under UV light for 30 minutes. Subsequently, 100 µL of bacterial suspension was pipetted onto each membrane and antibacterial performance was measured until 24 hours of contact time with 2 hours interval. At each time point, the membrane and the 100-µL of bacterial suspension were introduced to 5 ml of sterile distilled water and vortexed for 2 minutes to promote disaggregation of bacteria from the membranes. Antibacterial performance of the membranes was calculated in terms of *LRV* (how was LRV calculated here as compared to previous section?) as stated in Equation 4 previously. Experiment was performed in triplicates to account for repeatability.

RESULTS AND DISCUSSION

Morphology Analysis

The morphology of electrospun membranes is illustrated in Figure 2. Electrospun PAN membrane exhibited a randomly oriented, ultrafine, and well-uniformed structure (Figure 2a, e). Under the specified electrospinning conditions, the diameters of electrpsun PAN nanofibers highly populated within the range of 450−550 nm with an average diameter of 484 nm. Furthermore, incorporated ZnO (5 w/w %) nanoparticles did not affect the average fiber diameter of PAN, but formed minor agglomeration and clusters along the PAN fibers axis, which disturbed the rigidity of some of fibers (Figure 2b, f). Micrographs of electrospun PAN/Cs

(Figure 2c) and PAN/ZnO-Cs (Figure 2d) membranes illustrated that chitosan layer has almost a fibrous structure in most areas while spots with film-like structure were also observed, attributed to high viscosity of chitosan solution which hindered the smoothness of electrospinning process. It can be seen that chitosan nanofibers are well overlapped on PAN fibers (Figure 2g) and PAN/ZnO (Figure 2h) fibers while forming linkages between them. These linkages can provide improvements in mechanical and thermal properties of PAN and PAN/ZnO membranes, which will be further discussed.

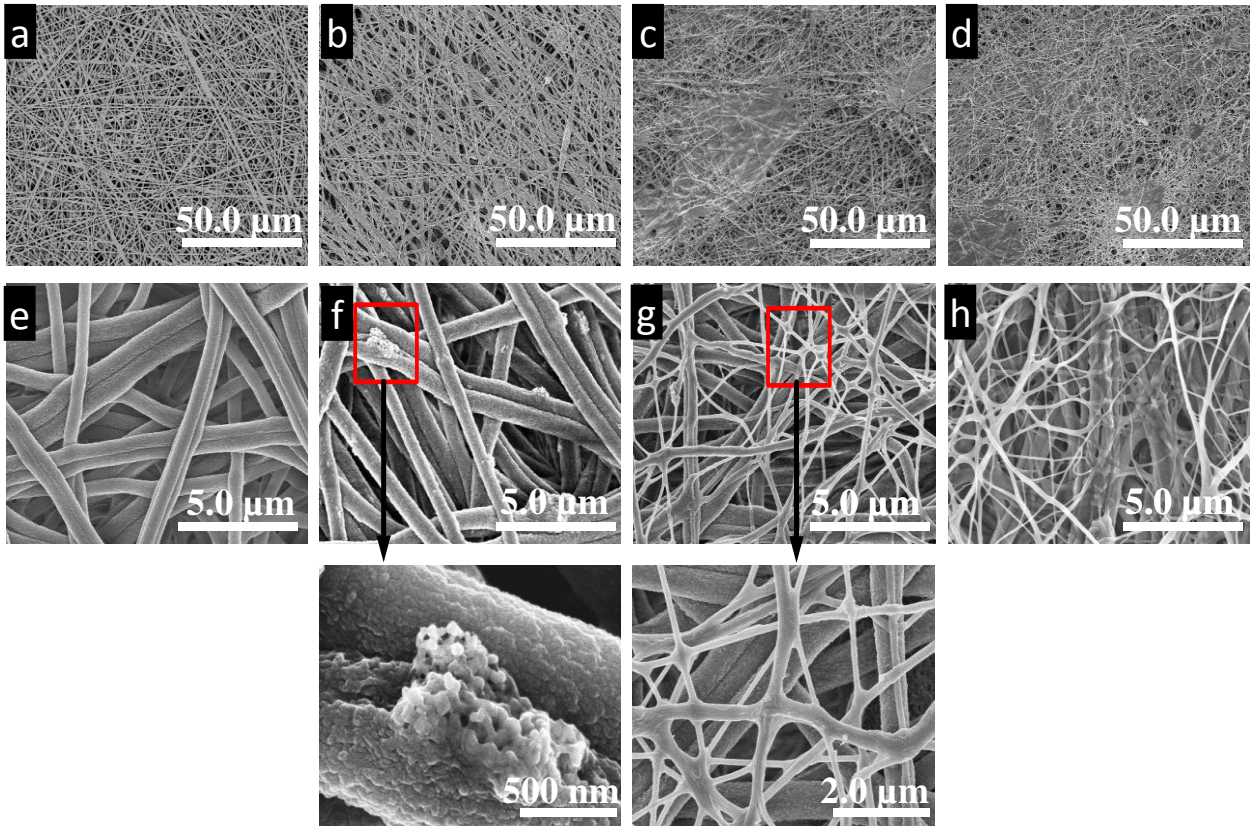

Figure 2.FESEM micrographs of electrospun nanofibrous membranes at low (top row) and high (bottom row) magnifications. Electrospun (a,e) PAN, (b, f) PAN/ZnO, (c, g) PAN-Cs, (d, h) PAN/ZnO-Cs membranes. Micrographs below f and g are magnified to reveal the arrangement of the fibers and nanoparticles.

Figure 3 shows a FESEM image of the cross-section of an electrospun PAN/ZnO-Cs membrane. It can be seen that PAN membrane is covered by a thin layer of electrospun chitosan which appears somewhat less fibrous and less porous in comparison to the electropsun PAN membrane.

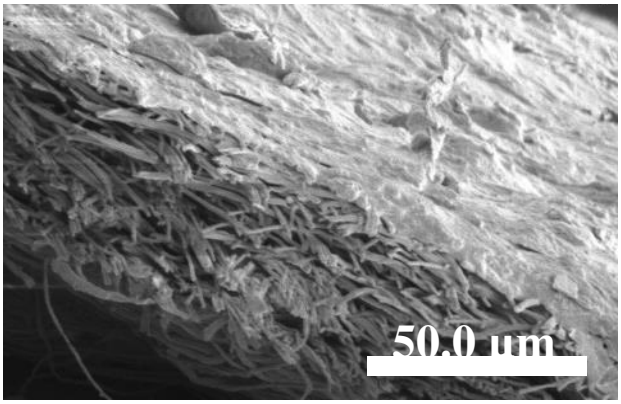

Figure 3. FESEM micrographs of a cross-section of an electrospun PAN/ZnO-Cs membrane.

STEM micrographs of electrospun PAN/ZnO membranes reveal the presence of ZnO nanoparticle clusters along the surface of the PAN nanofibers (Figure 4a-c). Agglomerates of ZnO nanoparticles may have a negative effect on the mechanical properties of the electrospun PAN membranes.

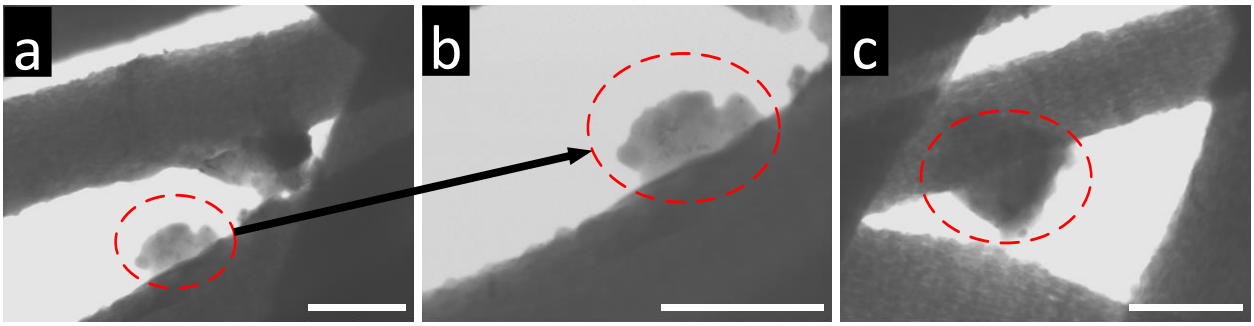

Figure 4. STEM micrographs of electrospun PAN/ZnO membranes. Scale bars represent 500 nm.

In summary, the following structural hierarchical levels can be identified in the membranes of PAN, PAN/ZnO, PAN-Cs and PAN/ZnO-Cs: (1) the fibrous structure of the (i.e. mono-layer versus bi-layer) membrane (Figure 3); (2) the structure of the nanofibres (Figure 2 e-h) and (3) the arrangement of the ZnO particles on the PAN nanofibres (the magnified view of Figure 2 g).

Fourier transform infrared (FTIR) analysis

Figure 5 shows the FTIR spectra of electrospun PAN, PAN-Cs, PAN/ZnO and PAN/ZnO-Cs membranes along with the raw materials of chitosan, ZnO and PAN. In the FTIR spectrum of chitosan (Figure 5b), characteristic peaks of carbonyl stretching of the secondary amide band (amide I) and the N–H bending of the primary amino groups were observed at 1654 cm^{-1} and 1590 cm^{-1}, respectively. Furthermore, characteristic peaks of saccharide structure of chitosan were observed at 1149 cm^{-1} and 893 cm^{-1} [33]. FTIR spectra of electrospun PAN and PAN/ZnO (Figure 5d-e) membranes indicated a shift in vibrational bands of C−N groups from 1072 cm^{-1} to 1041 cm^{-1} attributed to strong drawing forces occurred in the electrospinning process which led to structural modification.

Major peak shifts were observed in electrospun membranes containing the chitosan layer (Figure 5f-g). Overlapping of C-O and C-N stretching vibrations of chitosan and PAN increased the intensity of the peak at 1065 cm^{-1}, while intensity reduced in characteristic peak of saccharide structure of chitosan at 1026 cm^{-1}. Furthermore, intensity of CH_2 symmetrical bending vibration of PAN at 1452 cm^{-1} along with C≡N stretching at 2242 cm^{-1} were decreased in electrospun membranes coated with the chitosan layer. These chemical interactions between PAN and chitosan macromolecules may lead to improvement in mechanical properties of PAN/Cs membrane.

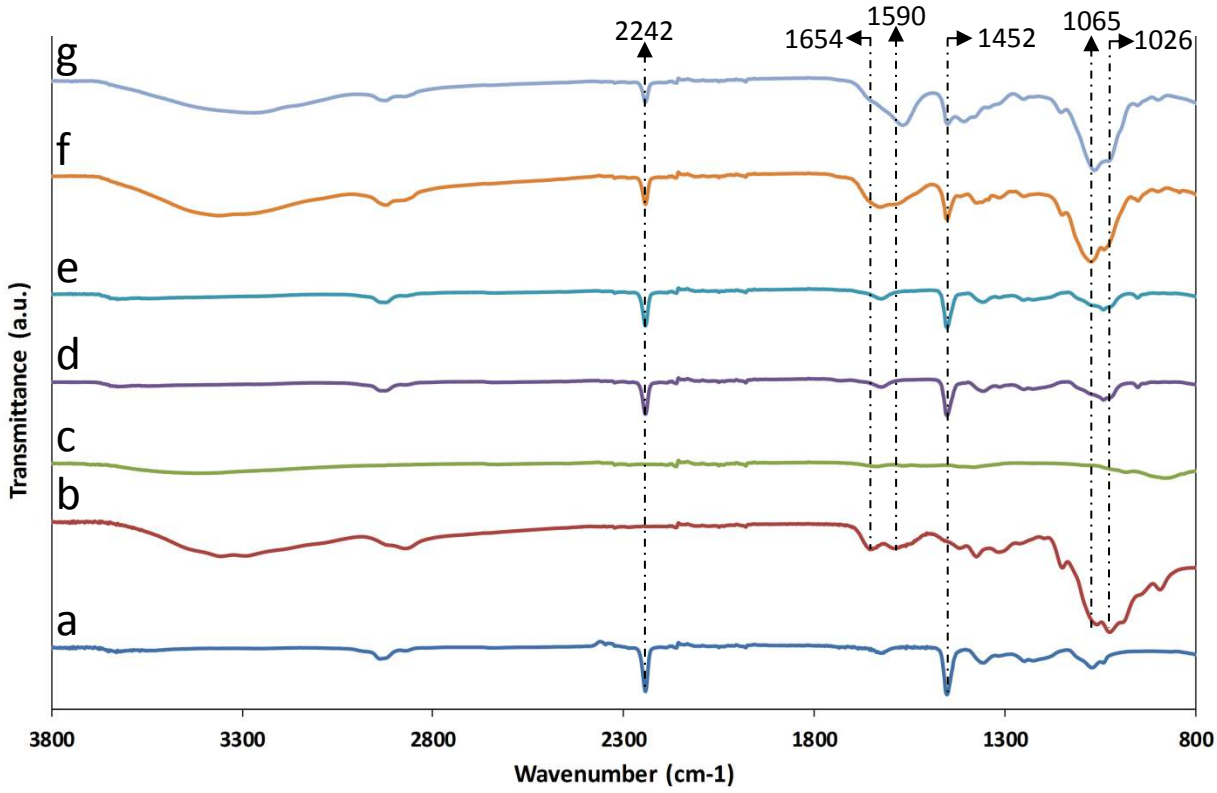

Figure 5.FTIR spectra of: (a) PAN powder, (b) pure chitosan powder, (c) pure ZnO powder, (d) as-spun PAN nanofibers, (e) as-spun PAN/ZnO nanofibers, (f) as-spun PAN/Cs nanofibers, (g) as-spun PAN/ZnO-Cs nanofibers.

Tensile tests

Significant differences ($p < 0.05$) were observed for the respective mechanical properties, namely tensile strength, elastic modulus and elongation at break, among the four different types of membranes, i.e. PAN, PAN/ZnO, PAN-Cs and PAN/ZnO-Cs. The detailed results concerning the differences are discussed in the following paragraphs. Table 1 summarizes the results of the tensile tests.

Addition of a chitosan layer (i.e. to PAN in the absence of ZnO) appreciably increases the tensile strength and elastic modulus of PAN membrane by 74% and 32%, respectively. As observed in the morphology discussion, chitosan nanofibers were positioned mostly in between

the PAN fibers and created linkages between them, leading to enhancement in rigidity of the membranes as well as ease in stress transfer at the interface, implicating the respective increases in elastic modulus and tensile strength. However, tensile strengths of electrospun PAN and PAN/Cs membranes incorporated with ZnO nanoparticles are respectively 34% and 43%, lower than PAN membranes; the elastic moduli of these ZnO nanoparticles incorporated membranes are respectively 18 and 28% lower than PAN membranes. As mentioned in the morphology discussion, incorporation of ZnO nanoparticles led to formation of agglomerations on the surface of the PAN nanofibers. Existence of these clusters impaired the effective load transfer from the polymer matrix to the fillers by reducing the surface area in contract with nanoparticles and becoming the site of stress concentration, resulting in poor stress transfer at the interface and ultimately reduction of mechanical properties [34]. Moreover, agglomeration of ZnO nanoparticles would also lead to the disruption of PAN polymeric chains, reducing the rigidity of nanofibers.

With regards to the elongation at break, incorporation of ZnO nanoparticles and addition of the chitosan layer to the electrospun PAN membranes leads to a composite membrane with reduced elongation at break as compared to PAN membranes. Thus the elongation at break for PAN/ZnO and PAN/ZnO-Cs are 70% and 60%, respectively, lower than PAN membranes. The fracture toughness (in terms of strain energy density) of the membrane are of order of one-half the product of tensile strength and elongation at break; for PAN, PAN/ZnO and PAN/ZnO-Cs membranes, order of magnitude estimates of the strain energy density to fracture yield 0.6, 0.1 and 0.2 MPa, respectively. Thus, it can be seen that incorporation of 5 wt% ZnO nanoparticles dramatically reduces the fracture toughness of the membrane, attributing to the agglomeration of nanoparticles. On the other hand, it must be mentioned that PAN/ZnO-Cs membrane has almost similar tensile strength and elastic modulus with pure PAN membrane.

Table 1. Mechanical Properties of Electrospun Membranes

Sample	Tensile strength (MPa)	Elastic modulus (GPa)	Elongation at break (%)
PAN	13.0 ± 0.7	0.56 ± 0.10	9.0 ± 1.6

PAN/ZnO	8.5 ± 1.3	0.46 ± 0.10	2.6 ± 1.2
PAN/Cs	22.7 ±2.4	0.74 ± 0.20	8.5 ± 2.2
PAN/Cs/ZnO	12.9 ± 1.8	0.53 ± 0.10	3.5 ± 1.3

X-ray Diffraction (XRD) Analysis

Crystalline structure of electrospun PAN membranes with chitosan layer and incorporated ZnO nanoparticles have been investigated using X-ray diffractograms and represented in Figure 6. PAN powder (Figure 6a) exhibited two equatorial peaks. The primary equatorial (100) peak at 2θ = 16.8° corresponds to a spacing of 5.25 Å while the weaker reflection (110) at 2θ = 29.5° corresponds to a spacing of 3.05 Å. The d-spacing ratio of these two peaks (1.72) is very close to $\sqrt{3}$:1 indicating hexagonal packing of the rod-like PAN chains [35]. Furthermore, chitosan powder (Figure 6b) exhibited a broad peak at 2θ = 10.9° (d = 8.110Å) and a strong peak at 2θ = 19.8° (d = 4.489Å). Moreover, ZnO powder (Figure 6c) showed three typical peaks at 2θ=31.5° (1 0 0) (d =2.831Å), 34.2° (0 0 2) (d =2.617Å), 36° (1 0 1) (d =2.488Å) indexing the hexagonal ZnO crystal structure while the sharpness of the peaks revealed a highly crystallized wurtzite structure [36].

XRD pattern of electrospun PAN membrane (Figure 6d) revealed the existence of PAN equatorial peak at 2θ = 16.8°. Electrospun PAN/ZnO membrane (Figure 6e) possessed both PAN and ZnO typical peaks. However, peak shifts were observed in ZnO peaks from 31.5° to 31.69°, 34.2° to 34.36° and 36° to 36.23°, implying that the lattice constant of ZnO crystal has somewhat changed, possibly due to drawing forces applied during the electrospinning process. XRD patterns of electrospun PAN/Cs (Figure 6f) and PAN/Cs/ZnO (Figure 6g) membranes showed a broad peak at 2θ = 12.38° contributed by chitosan nanofibers (shifted from 2θ = 10.9°) as well as a weak reflection at 2θ = 16.8° attributed by PAN nanofibers. It must be said that typical peaks of ZnO were not detected in XRD pattern of electrospun PAN/Cs/ZnO membrane. This could be

attributed to high density of chitosan nanofibers which covered the PAN/ZnO nanofibrous membrane, leading to their absence in the PAN/Cs/ZnO diffractograms.

Reflection peaks of all electrospun membranes (Figure 6d-g) were broad and weak compared to their raw materials, indicating that the crystalline microstructures of the electrospun membrane were not developed during the electrospinning process. The rapid evaporation of the solvent from the jet along with the rapid structure configuration, which occurs within milliseconds (~50 ms) leads to less developed structures in the fibers. The rapid solvent evaporation reduces the jet temperature and consequently, the molecules that are aligned along the fiber axis have less time to realign themselves, leading to less favorable packing. For the majority of semi-crystalline polymers, the stretched chains under high elongation rate do not get enough time to form crystalline lamellae, which yields to lesser crystallinity. Thus, the crystallinity in the fibers is thereby affected by the rate of solvent evaporation [37,38].

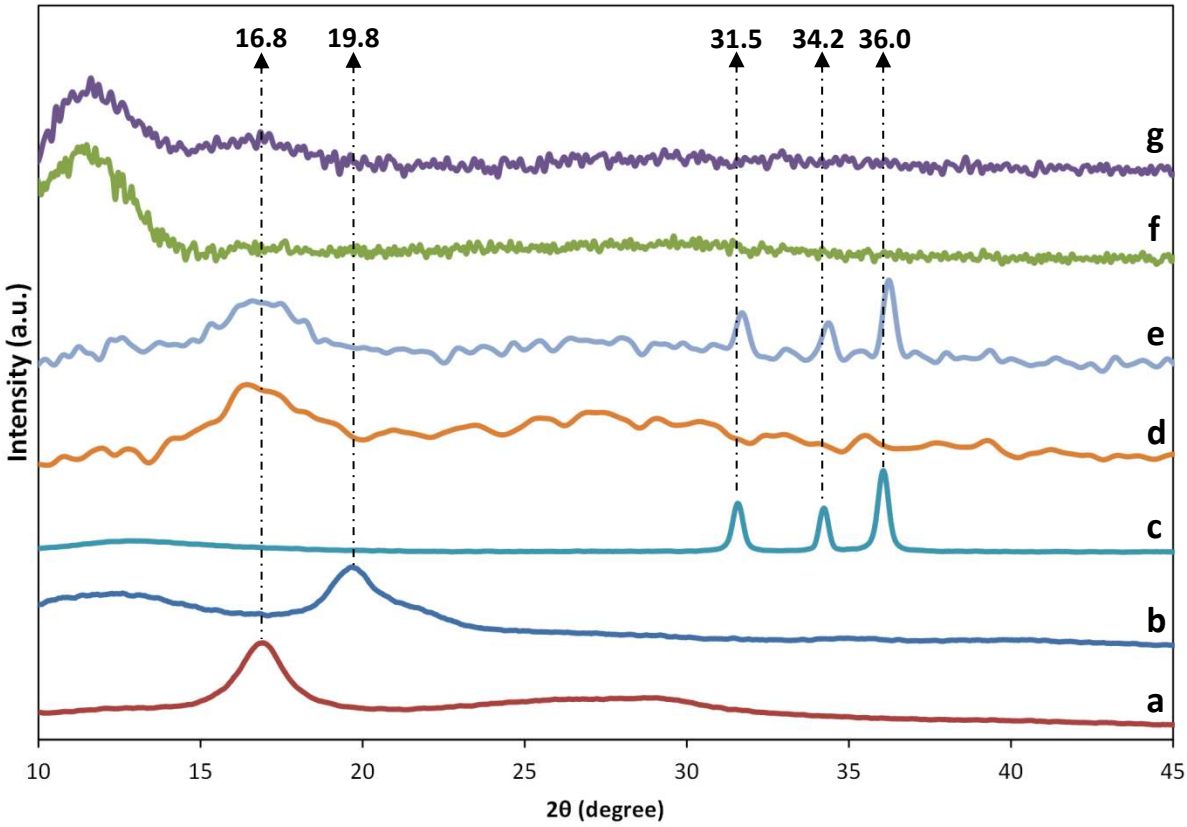

Figure 6. X-ray diffraction patterns of: (a) PAN powder, (b) pure chitosan powder, (c) pure ZnO powder, (d) as-spun PAN nanofibers, (e) as-spun PAN/ZnO nanofibers, (f) as-spun PAN/Cs nanofibers and (g) as-spun PAN/Cs/ZnO nanofibers.

Permeability and Porosity Analysis

Pure water flux rates of electrospun membranes measured by dead-end filtration cell have been summarized in Table 2. Incorporation of ZnO into electrospun PAN membranes increased the water permeability by 71%. This could be attributed to the increase in the number of internal nanochannels due to inclusion of ZnO nanoparticles. Disruption of polymer chains resulted from incorporation of ZnO nanoparticles could introduce nanoscaled cavities which provide additional pathways for water permeation, leading to improvement in water permeability of membranes. Similar results were reported by Wang *et al*. [39] , indicating the improvement in water flux of electrospun PVA membranes by incorporation of multi-walled carbon nanotubes (MWNTs). Conversely, it can be seen from Table 2 that addition of the chitosan layer dramatically decreased the permeate flux (i.e. the volume flowing through the membrane per unit area per unit time) of electrospun PAN membranes by 97%. This could be due to low surface porosity of electrospun chitosan layer compared to electrospun PAN membrane which provides fewer accessible pores for water, resulting in reduction in permeate flux. In case of electrospun PAN/Cs/ZnO membrane, although addition of chitosan layer decreased the permeate flux, but existence of ZnO nanoparticles let to 400% increase in flux rate of this membrane compared to PAN/Cs membrane, attributed to increase in number of internal nanochanels due to incorporation of ZnO nanoparticles.

Table 2 presents the porosity measurements of electrospun membranes. Porosity of electrospun PAN membrane was measured to be 75.4%, which is in the range of values reported in literature [40–42]. Addition of electrospun chitosan layer reduced the porosity value of electrospun PAN membranes by almost 12%. This was expected since addition of chitosan layer reduced the surface porosity of electrospun PAN membrane and reduced the gaps between fibers by providing linkages between them. It must be mentioned that incorporation of ZnO also reduced the porosity of PAN membranes by 1.2%, which could be considered negligible.

Table2. Porosity and pure water permeate flux of electrospun membranes.

Sample	Thickness (mm)	Pure water Flux ($L.m^{-2}h^{-1}$)	Porosity (%)
PAN	0.042	12244	75.4
PAN/ZnO	0.050	20991	74.2
PAN/Cs	0.062	293	63.7
PAN/Cs/ZnO	0.072	1469	61

Heavy metal ion adsorption

Heavy metal ion adsorption properties of electrospun membranes have been shown in Table 3. Incorporation of ZnO nanoparticles to electrospun PAN membranes improved the Cr (III) removal efficiency from 4 to 34%. This could be explained by Cr (III) attraction to negative sites on surface hydroxyl groups of ZnO [43, 44]. Additionally, adsorption of Cr (III) ions might take place when they move through either the pores of ZnO mass or through channels of the crystal lattice [45]. Hence, polar nature of ZnO surface (positively charged Zn ion and negatively charged O-ion) as well as their porous structure are the main parameters in adsorption properties of ZnO [46]. In a similar study performed by Hallaji *et al.* [47] electrospun polyvinyl alcohol (PVA) membranes reinforced by ZnO nanoparticles were utilized for adsorption of heavy metals from aqueous solution. Results indicated that the membrane had the capacity values of 370.86, 162.48 and 94.43 mg/g for sorption of U(VI), Cu(II) and Ni(II) ions, respectively. These results along with results obtain in this research indicates the high potential of electrospun membranes reinforced by ZnO nanoparticles to be used in water filtration applications.

Similarly, addition of chitosan layer to electrospun PAN membranes increased the Cr (III) removal efficiency to 43%. This could be attributed to high surface area, inter and intra

pores, as well as large number of the chelating groups of chitosan. It has been reported that chitosan has the highest chelating ability in comparison to other natural polymers owing to the amine and hydroxyl functional groups in its structure [48]. More specifically, the amine group (—NH_2) as one of chitosan organic compounds, is known to be very effective in removing heavy metals via chelating cationic metal ions and/or adsorbing anionic metal species through electrostatic interactions with protonated amino groups (—NH_3^+) or via hydrogen bonding [45]. Adsorption properties of electrospun chitosan membranes have been widely studied previously [49,50]. For instance, Haider *et al*. [20] examined the Cu(II) and Pb(II) adsorption performance of electrospun chitosan membranes. Results indicated high adsorption capacity of chitosan membranes which could be applied to adsorb (or neutralize) toxic metal ions and microbes.

Electrospun PAN/Cs/ZnO membrane has the highest adsorption performance among the tested membranes in this study with removal efficiency value of 75%. As discussed in detail earlier, both chitosan and ZnO have significant adsorption properties. Therefore, this membrane benefited from the combination of adsorption mechanisms which have been provided by both chitosan and ZnO.

Table3. Adsorption Performance of Electrospun Membranes

Membrane	Removal efficiency (%)
PAN	4
PAN/ZnO	34
PAN-Cs	43
PAN/ZnO-Cs	75

Bacteria Filtration

Figure 7 shows bacteria filtration performance of electrospun membranes. Log reduction value of electrospun PAN membrane was around 4 for both *E. coli* and *E. faecalis*. It is known that *E. coli* has a cylindrical shape with a longitude length of 1.5 µm while cocci shaped *E.faecalis* is 1µm long with diameter of 0.6 µm [51]. Entrapment of bacteria cells is the key filtration mechanism in electrospun PAN membranes, since the average pore size of this membrane (300-700 nm) is smaller than the size of both bacteria types. Dramatic improvements in bacteria filtration performance were observed in electrospun membranes with chitosan coating layer. For instance, electrospun PAN/Cs membrane exhibited log reduction of 6.6 and 6.2 against *E.coli* and *E.faecalis*, respectively. These values indicate that PAN/Cs membrane displayed excellent bacteria filtration performance, leading to reduction in initial bacteria concentration by more than 99 %. As mentioned in the section on morphology, chitosan nanofibers provide linkages between PAN nanofibers, which lead to reduction in surface porosity of the membrane. Hence, electrospun membranes with chitosan layer have smaller pore sizes (Table 2), leading to improvement in their filtration performance exhibited through size exclusion mechanism. However, it can be seen that incorporation of ZnO nanoparticles to electrospun PAN and PAN/Cs membranes somewhat reduced the bacteria filtration performance of these membranes. This could be attributed to the inhomogeneity and reduced rigidity of the PAN fibers due to ZnO agglomeration, implicating the possible formation of additional pathways for bacteria which facilitated their movement through the membrane.

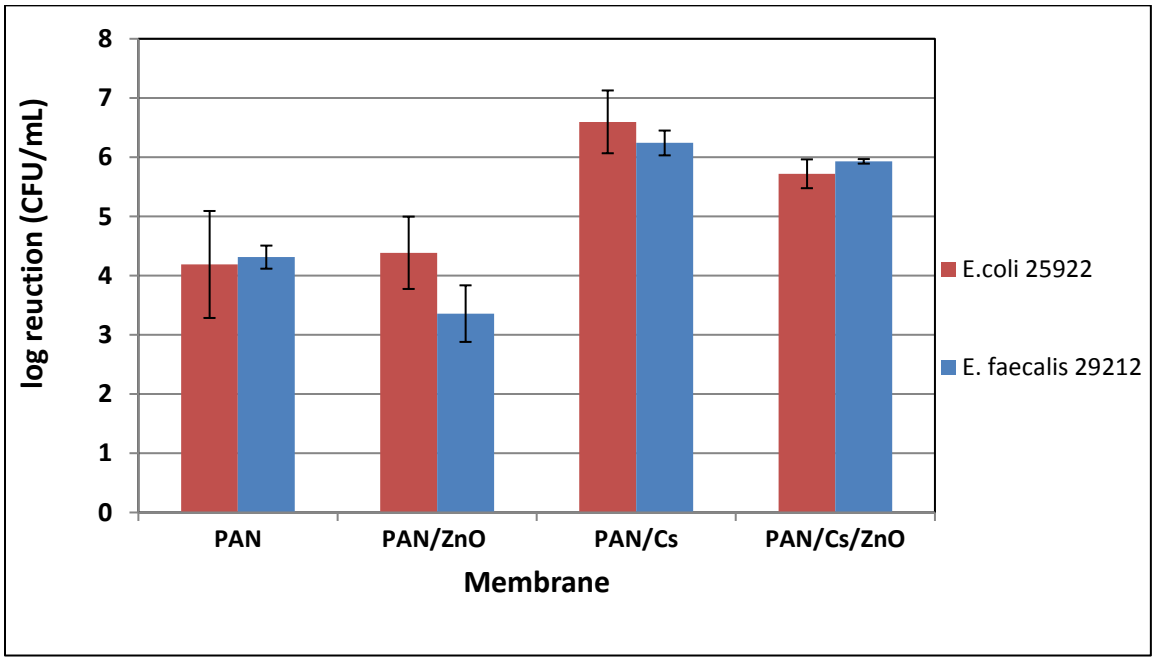

Figure 7. Bacteria filtration performance of electrospun membranes. (the argument in LRV is unitless because it is a ratio)

Figure 8 shows the FESEM micrographs of trapped *E.coli* and *E.feacalis* on the electrospun PAN and PAN/ZnO-Cs membranes. As shown in Figures 8b and d, larger bacteria population was observed on the PAN/ZnO-Cs membranes in comparison to PAN membranes (Figure 8a,c), indicating the significant improvement provided by chitosan layer in filtration performance of membranes.

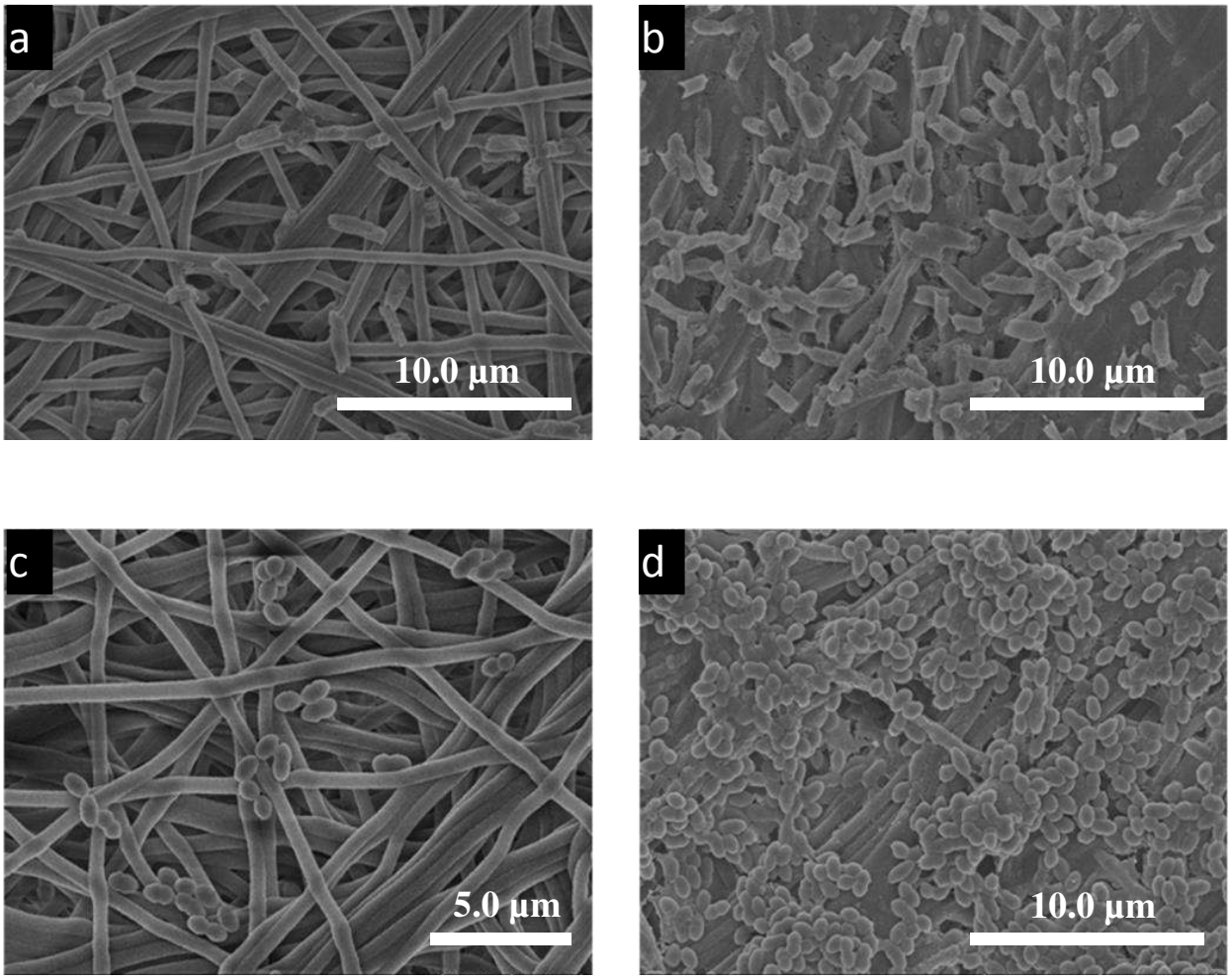

Figure 8.FE-SEM micrographs of electrospun (a) PAN and (b) PAN/ZnO-Cs membranes after filtration of *E.coli* along with micrographs of electrospun (c) PAN and (d) PAN/ZnO-Cs membranes after filtration of *E.feacalis.*

Antibacterial analysis

Figure 9 shows time-kill curves of electrospun membranes against *E. coli*. It is seen that the LRV increases with time; the increase is most rapid for PAN/ZnO-Cs, followed by PAN/ZnO, PAN-Cs and PAN membranes. However, only the LRV for the PAN/ZnO-Cs and PAN/ZnO membranes converges to a constant by the end of the 24-h experiment. By fitting a

simple threshold model to the converged curves, it was found that the tipping point, leading to the reduction in the bacteria population, is 2 h and 4 h for PAN/ZnO-Cs and PAN/ZnO, respectively. Thus, the PAN/ZnO-Cs exhibits the best antibacteria action, followed by PAN/ZnO membrane. On the other hand, the (pure) PAN membranes (as well as the PAN-Cs) appeared to have very little antibacteria effect. This was to be expected since these membranes do not have any known mechanism to kill the bacteria. Therefore, under the application conditions, microorganism species can readily contaminate PAN membranes, resulting in serious microorganism buildups. Of note, addition of the chitosan layer to electrospun PAN/ZnO membranes resulted in 2 orders of magnitude increase in LRV at 4 h; in other words, the reduction in bacteria concentration after 4 hours is 2 orders of magnitude greater than the PAN/ZnO membrane. This is due to interaction between positive charges presented by the amine functionalities of chitosan and negatively charged microbial cell membranes, which leads to the leakage of proteinaceous and other intracellular constituents in bacteria and eventually cell death.

Dramatic improvement in antibacterial performance of the membranes was observed by incorporation of ZnO nanoparticles. Electrospun PAN/ZnO membranes caused 6 orders of magnitude reduction in bacteria concentration after 8 hours of contact time (more than 3 orders of magnitude occurred after the first 3 hours of the contact). Three mechanisms have been suggested to contribute in antimicrobial properties of ZnO nanoparticles. Highly active free radicals such as hydroxyl radicals (OH), superoxide anion (O_2^-) and perhydroxyl radicals (HO_2) are formed from electron–hole pairs generated by ZnO nanoparticles under light (both UV and visible light) irradiation[55]. These radicals are capable of penetrating into the bacterial cells and cause complete destruction. Alternatively, the release of Zn^{2+} ions may interact with microbial membrane to cause structural change and permeability, as well as interacting with microbial nucleic acids to prevent microbial replication[24]. Furthermore, electrostatic force between the negatively charged bacteria cells with positive sites of ZnO nanoparticles could result in cell membrane damage. Of these mechanisms, the most likely explanation for the antibacterial activity of PAN/ZnO membrane is the presence of active radical oxygen species of superoxide anion (O_2^-) and their strong oxidizing interactions with bacterial cells.

Moreover, existence of both chitosan layer and ZnO nanoparticles in electrospun PAN/ZnO-Cs membrane has further improved the antimicrobial efficacy. On one hand, ZnO nanoparticles are potent antimicrobial agents that are able to kill microbial cells and on the other hand, the amidoxime groups on the chitosan layer possess antimicrobial functionality through their ionic inter-actions with negatively charged surface of bacteria. Therefore, the combination of amidoxime functional groups and ZnO nanoparticles into one membrane provided synergetic effects on antibacterial efficacy.

In this study, the concentration of bacterial challenge was significantly greater than any condition present in natural environmental situations, signifying that the reduction observed within the 24-h time period may be translated to a dramatically extended filter lifetime for real-world conditions.

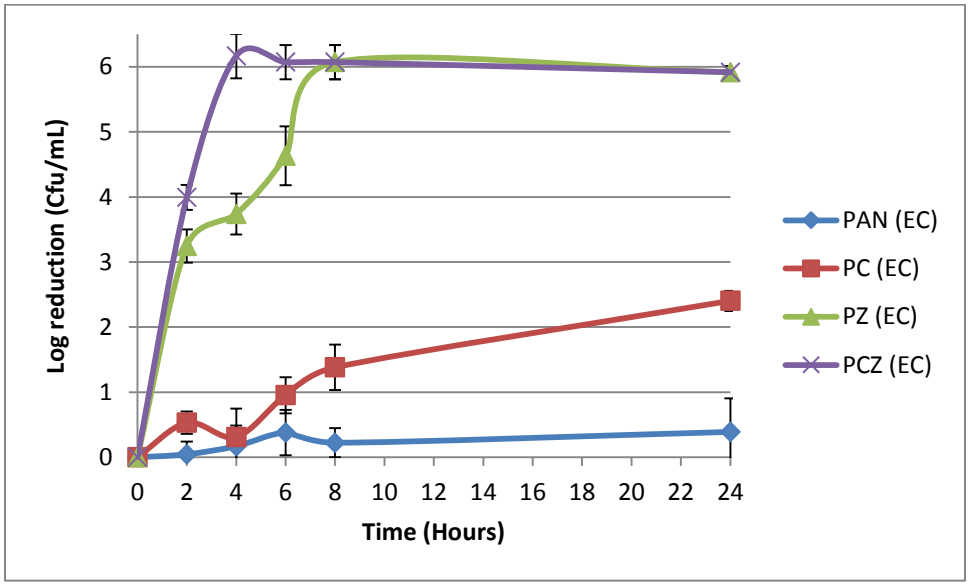

Figure 9. Time-kill curves of electrospun membranes against *E. coli*. (the argument in LRV is unitless because it is a ratio)

CONCLUSION

Electrospun nanofibrous membranes were successfully fabricated by polyacrylonitrile (PAN) functionalized by zinc oxide (ZnO) nanoparticles and a layer of electrospun chitosan (Cs). In order to evaluate the effect of ZnO and Cs on properties of electrospun PAN membrane, their morphology, mechanical stability and water filtration performance were characterized. Morphological analysis revealed the highly porous structure of nanofibrous PAN membranes while the thin layer of Cs coating displayed a less fibrous but smooth structure. Mechanical properties revealed that addition of the Cs layer increased the tensile strength and young modulus of the PAN membranes by 74% and 32%, respectively. Furthermore, incorporation of ZnO nanoparticles along with Cs layer increased the Cr (III) adsorption of the PAN membranes and led to a removal efficiency of 75%. Moreover, bacteria filtration via PAN/Cs membranes achieved values higher than 6 log reduction towards *Escherichia coli* and *Enterococcus faecalis*, while antibacterial assay demonstrated that PAN/ZnO-Cs membranes exhibits antibacterial action and completely killed all the bacteria in the first 3 hours. This indicates the self-cleaning property of PAN/ZnO-Cs membranes to remove bacteria upon filtration and reduces membrane biofouling resistance. Furthermore, results acquired from water permeability test indicated that the prepared membranes possessed adequate transport properties for typical membrane applications, which signifies the potential of these membranes to be used for water filtration applications, although further studies required in order to fabricate these membranes in an industrial scale.

REFERENCES

[1] Z. Ma, M. Kotaki, S. Ramakrishna, Electrospun cellulose nanofiber as affinity membrane, J. Memb. Sci. 265 (2005) 115–123. doi:http://dx.doi.org/10.1016/j.memsci.2005.04.044.

[2] R. GOPAL, S. KAUR, Z. MA, C. CHAN, S. RAMAKRISHNA, T. MATSUURA, Electrospun nanofibrous filtration membrane, J. Memb. Sci. 281 (2006) 581–586. doi:10.1016/j.memsci.2006.04.026.

[3] R. Gopal, S. Kaur, C.Y. Feng, C. Chan, S. Ramakrishna, S. Tabe, et al., Electrospun nanofibrous polysulfone membranes as pre-filters: Particulate removal, J. Memb. Sci. 289 (2007) 210–219. doi:http://dx.doi.org/10.1016/j.memsci.2006.11.056.

[4] H. Ma, B.S. Hsiao, B. Chu, Functionalized electrospun nanofibrous microfiltration membranes for removal of bacteria and viruses, J. Memb. Sci. 452 (2014) 446–452. doi:http://dx.doi.org/10.1016/j.memsci.2013.10.047.

[5] S.K. Nataraj, K.S. Yang, T.M. Aminabhavi, Polyacrylonitrile-based nanofibers—A state-of-the-art review, Prog. Polym. Sci. 37 (2012) 487–513. doi:10.1016/j.progpolymsci.2011.07.001.

[6] M. Botes, T.E. Cloete, The potential of nanofibers and nanobiocides in water purification., Crit. Rev. Microbiol. 36 (2010) 68–81. doi:10.3109/10408410903397332.

[7] K. Yoon, B.S. Hsiao, B. Chu, High flux ultrafiltration nanofibrous membranes based on polyacrylonitrile electrospun scaffolds and crosslinked polyvinyl alcohol coating, J. Memb. Sci. 338 (2009) 145–152. doi:10.1016/j.memsci.2009.04.020.

[8] S. Kaur, S. Sundarrajan, D. Rana, T. Matsuura, S. Ramakrishna, Influence of electrospun fiber size on the separation efficiency of thin film nanofiltration composite membrane, J. Memb. Sci. 392–393 (2012) 101–111. doi:http://dx.doi.org/10.1016/j.memsci.2011.12.005.

[9] K. V Harish Prashanth, R.N. Tharanathan, Chitin/chitosan: modifications and their unlimited application potential—an overview, Trends Food Sci. Technol. 18 (2007) 117–131. doi:http://dx.doi.org/10.1016/j.tifs.2006.10.022.

[10] P.K. Dutta, S. Tripathi, G.K. Mehrotra, J. Dutta, Perspectives for chitosan based antimicrobial films in food applications, Food Chem. 114 (2009) 1173–1182. doi:http://dx.doi.org/10.1016/j.foodchem.2008.11.047.

[11] R. Jayakumar, M. Prabaharan, S. V Nair, H. Tamura, Novel chitin and chitosan nanofibers in biomedical applications, Biotechnol. Adv. 28 (2010) 142–150. doi:http://dx.doi.org/10.1016/j.biotechadv.2009.11.001.

[12] J.-P. Chen, G.-Y. Chang, J.-K. Chen, Electrospun collagen/chitosan nanofibrous membrane as wound dressing, Colloids Surfaces A Physicochem. Eng. Asp. 313–314 (2008) 183–188. doi:http://dx.doi.org/10.1016/j.colsurfa.2007.04.129.

[13] X.-J. Huang, D. Ge, Z.-K. Xu, Preparation and characterization of stable chitosan nanofibrous membrane for lipase immobilization, Eur. Polym. J. 43 (2007) 3710–3718. doi:http://dx.doi.org/10.1016/j.eurpolymj.2007.06.010.

[14] K. Desai, K. Kit, J. Li, P. Michael Davidson, S. Zivanovic, H. Meyer, Nanofibrous chitosan non-wovens for filtration applications, Polymer (Guildf). 50 (2009) 3661–3669.

[15] D. Zeng, J. Wu, J.F. Kennedy, Application of a chitosan flocculant to water treatment, Carbohydr. Polym. 71 (2008) 135–139. doi:http://dx.doi.org/10.1016/j.carbpol.2007.07.039.

[16] M. Pakravan, M.-C. Heuzey, A. Ajji, A fundamental study of chitosan/PEO electrospinning, Polymer (Guildf). 52 (2011) 4813–4824. doi:http://dx.doi.org/10.1016/j.polymer.2011.08.034.

[17] Y.-T. Jia, J. Gong, X.-H. Gu, H.-Y. Kim, J. Dong, X.-Y. Shen, Fabrication and characterization of poly (vinyl alcohol)/chitosan blend nanofibers produced by electrospinning method, Carbohydr. Polym. 67 (2007) 403–409. doi:http://dx.doi.org/10.1016/j.carbpol.2006.06.010.

[18] N. Bhattarai, D. Edmondson, O. Veiseh, F.A. Matsen, M. Zhang, Electrospun chitosan-based nanofibers and their cellular compatibility, Biomaterials. 26 (2005) 6176–6184. doi:http://dx.doi.org/10.1016/j.biomaterials.2005.03.027.

[19] A. Cooper, R. Oldinski, H. Ma, J.D. Bryers, M. Zhang, Chitosan-based nanofibrous membranes for antibacterial filter applications, Carbohydr. Polym. 92 (2013) 254–259. doi:http://dx.doi.org/10.1016/j.carbpol.2012.08.114.

[20] S. Haider, S.-Y. Park, Preparation of the electrospun chitosan nanofibers and their applications to the adsorption of Cu(II) and Pb(II) ions from an aqueous solution, J. Memb. Sci. 328 (2009) 90–96. doi:http://dx.doi.org/10.1016/j.memsci.2008.11.046.

[21] R. Augustine, H. Malik, D. Singhal, A. Mukherjee, D. Malakar, N. Kalarikkal, et al., Electrospun polycaprolactone/ZnO nanocomposite membranes as biomaterials with antibacterial and cell adhesion properties, J. Polym. Res. 21 (2014) 1–17. doi:10.1007/s10965-013-0347-6.

[22] W.K. Son, J.H. Youk, W.H. Park, Antimicrobial cellulose acetate nanofibers containing silver nanoparticles, Carbohydr. Polym. 65 (2006) 430–434. doi:http://dx.doi.org/10.1016/j.carbpol.2006.01.037.

[23] S. Lee, Multifunctionality of layered fabric systems based on electrospun polyurethane/zinc oxide nanocomposite fibers, J. Appl. Polym. Sci. 114 (2009) 3652–3658. doi:10.1002/app.30778.

[24] Y. Wang, Q. Zhang, C. Zhang, P. Li, Characterisation and cooperative antimicrobial properties of chitosan/nano-ZnO composite nanofibrous membranes, Food Chem. 132 (2012) 419–427. doi:http://dx.doi.org/10.1016/j.foodchem.2011.11.015.

[25] A. Dasari, J. Quirós, B. Herrero, K. Boltes, E. García-Calvo, R. Rosal, Antifouling membranes prepared by electrospinning polylactic acid containing biocidal nanoparticles, J. Memb. Sci. 405–406 (2012) 134–140. doi:http://dx.doi.org/10.1016/j.memsci.2012.02.060.

[26] S. Anitha, B. Brabu, D. John Thiruvadigal, C. Gopalakrishnan, T.S. Natarajan, Optical, bactericidal and water repellent properties of electrospun nano-composite membranes of cellulose acetate and ZnO, Carbohydr. Polym. 97 (2013) 856–863. doi:http://dx.doi.org/10.1016/j.carbpol.2013.05.003.

[27] K.T. Shalumon, K.H. Anulekha, S. V Nair, S. V Nair, K.P. Chennazhi, R. Jayakumar, Sodium alginate/poly(vinyl alcohol)/nano ZnO composite nanofibers for antibacterial wound dressings, Int. J. Biol. Macromol. 49 (2011) 247–254. doi:http://dx.doi.org/10.1016/j.ijbiomac.2011.04.005.

[28] S.H. Hwang, J. Song, Y. Jung, O.Y. Kweon, H. Song, J. Jang, Electrospun ZnO/TiO2 composite nanofibers as a bactericidal agent, Chem. Commun. 47 (2011) 9164–9166. doi:10.1039/C1CC12872H.

[29] S. Singh, K. C., D. Bahadur, Functional Oxide Nanomaterials and Nanocomposites for the Removal of Heavy Metals and Dyes, Nanomater. Nanotechnol. (2013) 1. doi:10.5772/57237.

[30] X. Ma, Y. Wang, M. Gao, H. Xu, G. Li, A novel strategy to prepare ZnO/PbS heterostructured functional nanocomposite utilizing the surface adsorption property of ZnO nanosheets, Catal. Today. 158 (2010) 459–463. doi:http://dx.doi.org/10.1016/j.cattod.2010.07.013.

[31] Q.-Z. Zheng, P. Wang, Y.-N. Yang, D.-J. Cui, The relationship between porosity and kinetics parameter of membrane formation in PSF ultrafiltration membrane, J. Memb. Sci. 286 (2006) 7–11. doi:http://dx.doi.org/10.1016/j.memsci.2006.09.033.

[32] N. Daels, S. De Vrieze, I. Sampers, B. Decostere, P. Westbroek, A. Dumoulin, et al., Potential of a functionalised nanofibre microfiltration membrane as an antibacterial water filter, Desalination. 275 (2011) 285–290. doi:http://dx.doi.org/10.1016/j.desal.2011.03.012.

[33] M. Koosha, H. Mirzadeh, M.A. Shokrgozar, M. Farokhi, Nanoclay-reinforced electrospun chitosan/PVA nanocomposite nanofibers for biomedical applications, RSC Adv. 5 (2015) 10479–10487. doi:10.1039/C4RA13972K.

[34] D.W. Chae, B.C. Kim, Effects of zinc oxide nanoparticles on the physical properties of polyacrylonitrile, J. Appl. Polym. Sci. 99 (2006) 1854–1858. doi:10.1002/app.22533.

[35] Z. Bashir, S.P. Church, D. Waldron, Interaction of water and hydrated crystallization in water-plasticized polyacrylonitrile films, Polymer (Guildf). 35 (1994) 967–976. doi:http://dx.doi.org/10.1016/0032-3861(94)90940-7.

[36] X. Wang, M. Zhao, F. Liu, J. Jia, X. Li, L. Cao, C2H2 gas sensor based on Ni-doped ZnO electrospun nanofibers, Ceram. Int. 39 (2013) 2883–2887. doi:http://dx.doi.org/10.1016/j.ceramint.2012.09.062.

[37] A. Baji, Y.-W. Mai, S.-C. Wong, M. Abtahi, P. Chen, Electrospinning of polymer nanofibers: Effects on oriented morphology, structures and tensile properties, Compos. Sci. Technol. 70 (2010) 703–718. doi:10.1016/j.compscitech.2010.01.010.

[38] M. Makaremi, R. De Silva, P. Pasbakhsh, Electrospun Nanofibrous Membranes of Polyacrylonitrile/halloysite with Superior Water Filtration Ability, J. Phys. Chem. C. (2015). doi:10.1021/acs.jpcc.5b00662.

[39] X. Wang, X. Chen, K. Yoon, D. Fang, B.S. Hsiao, B. Chu, High flux filtration medium based on nanofibrous substrate with hydrophilic nanocomposite coating., Environ. Sci. Technol. 39 (2005) 7684–91. http://www.ncbi.nlm.nih.gov/pubmed/16245845 (accessed June 27, 2014).

[40] R. Wang, Y. Liu, B. Li, B.S. Hsiao, B. Chu, Electrospun nanofibrous membranes for high flux microfiltration, J. Memb. Sci. 392-393 (2012) 167–174. doi:10.1016/j.memsci.2011.12.019.

[41] L. Huang, S.S. Manickam, J.R. McCutcheon, Increasing strength of electrospun nanofiber membranes for water filtration using solvent vapor, J. Memb. Sci. 436 (2013) 213–220. doi:http://dx.doi.org/10.1016/j.memsci.2012.12.037.

[42] K. Yoon, B.S. Hsiao, B. Chu, High flux nanofiltration membranes based on interfacially polymerized polyamide barrier layer on polyacrylonitrile nanofibrous scaffolds, J. Memb. Sci. 326 (2009) 484–492. doi:http://dx.doi.org/10.1016/j.memsci.2008.10.023.

[43] S. Mahdavi, M. Jalali, A. Afkhami, Removal of heavy metals from aqueous solutions using Fe3O4, ZnO, and CuO nanoparticles, J. Nanoparticle Res. 14 (2012) 1–18. doi:10.1007/s11051-012-0846-0.

[44] Y. Kikuchi, Q. Qian, M. Machida, H. Tatsumoto, Effect of ZnO loading to activated carbon on Pb(II) adsorption from aqueous solution, Carbon N. Y. 44 (2006) 195–202. doi:http://dx.doi.org/10.1016/j.carbon.2005.07.040.

[45] C.-J. Li, S.-S. Zhang, J.-N. Wang, T.-Y. Liu, Preparation of polyamides 6 (PA6)/Chitosan@FexOy composite nanofibers by electrospinning and pyrolysis and their Cr(VI)-removal performance, Catal. Today. 224 (2014) 94–103. doi:http://dx.doi.org/10.1016/j.cattod.2013.11.034.

[46] S. Singh, K.C. Barick, D. Bahadur, Novel and Efficient Three Dimensional Mesoporous Zno Nanoassemblies for Envirnomental Remediation, Int. J. Nanosci. 10 (2011) 1001–1005. doi:10.1142/S0219581X11008654.

[47] H. Hallaji, A.R. Keshtkar, M.A. Moosavian, A novel electrospun PVA/ZnO nanofiber adsorbent for U(VI), Cu(II) and Ni(II) removal from aqueous solution, J. Taiwan Inst. Chem. Eng. 46 (2015) 109–118. doi:http://dx.doi.org/10.1016/j.jtice.2014.09.007.

[48] A.J. Varma, S. V Deshpande, J.F. Kennedy, Metal complexation by chitosan and its derivatives: a review, Carbohydr. Polym. 55 (2004) 77–93. doi:http://dx.doi.org/10.1016/j.carbpol.2003.08.005.

[49] L.-L. Min, Z.-H. Yuan, L.-B. Zhong, Q. Liu, R.-X. Wu, Y.-M. Zheng, Preparation of chitosan based electrospun nanofiber membrane and its adsorptive removal of arsenate from aqueous solution, Chem. Eng. J. 267 (2015) 132–141. doi:http://dx.doi.org/10.1016/j.cej.2014.12.024.

[50] M. Aliabadi, M. Irani, J. Ismaeili, H. Piri, M.J. Parnian, Electrospun nanofiber membrane of PEO/Chitosan for the adsorption of nickel, cadmium, lead and copper ions from aqueous solution, Chem. Eng. J. 220 (2013) 237–243.

[51] W. Kangwansupamonkon, W. Tiewtrakoonwat, P. Supaphol, S. Kiatkamjornwong, Surface modification of electrospun chitosan nanofibrous mats for antibacterial activity, J. Appl. Polym. Sci. 131 (2014) n/a–n/a. doi:10.1002/app.40981.

[52] P. Espitia, N. deFátimaFerreira Soares, J. dosReis Coimbra, N. de Andrade, R. Cruz, E. Medeiros, Zinc Oxide Nanoparticles: Synthesis, Antimicrobial Activity and Food Packaging Applications, Food Bioprocess Technol. 5 (2012) 1447–1464. doi:10.1007/s11947-012-0797-6.

[53] M. Ignatova, K. Starbova, N. Markova, N. Manolova, I. Rashkov, Electrospun nano-fibre mats with antibacterial properties from quaternised chitosan and poly(vinyl alcohol), Carbohydr. Res. 341 (2006) 2098–2107. doi:http://dx.doi.org/10.1016/j.carres.2006.05.006.

[54] C. Wang, F. Yang, H. Zhang, Fabrication of non-woven composite membrane by chitosan coating for resisting the adsorption of proteins and the adhesion of bacteria, Sep. Purif. Technol. 75 (2010) 358–365. doi:http://dx.doi.org/10.1016/j.seppur.2010.09.005.

[55] R.T. De Silva, P. Pasbakhsh, S.M. Lee, A.Y. Kit, ZnO deposited/encapsulated halloysite–poly (lactic acid) (PLA) nanocomposites for high performance packaging films with improved mechanical and antimicrobial properties, Appl. Clay Sci. 111 (2015) 10–20. doi:http://dx.doi.org/10.1016/j.clay.2015.03.024.